Effective viscosity and tearing rate of polymer networks in the presence of cross-link slip

William McFadden

University of Chicago, Biophysical Sciences Program, Chicago, IL 60615

(Dated: 1 January 2014)

Abstract

We are trying to describe long timescale rates of deformation in semi-flexible filament networks with transient cross-links. We have addressed the problem using a simplified model in which cross-links are allowed to slip past one another in a linear drag-like manner. This model gives a prediction for the long timescale effective viscosity of the medium that depends on network architecture and effective drag coefficient between filaments. We predict different modes of anomalous behavior when the network undergoes large strains that drive it into an anisotropic configuration. We have verified our solution using computational models of filaments undergoing shear and extensional stress. In addition, we attempt to derive a time constant for network tearing. In this model, we find that the inclusion of slip gives rise to varying levels of connectivity even when network architecture alone would predict a fully connected structure.

CONTENTS

I. INTRODUCTION

Cross-linked networks of semi-flexible polymers are a class of materials with poorly understood but highly interesting properties. They are often studied in conjunction with their important role in the formation of the cell cytoskeleton, the structural underpinning of eukaryotic life. In addition to the important role of these types in living organisms[7, 22], *in vitro* studies have revealed interesting mechanical properties of these composite networks on their own, which has spurred much interest in soft-matter physics[4].

A. Rheological Observations of Cross-link Dominated Response

A key area of inquiry in soft matter physics concerns the long timescale motion of cross-linked polymer networks as this may govern physiologically important behaviors[24].

The mechanics of semi-flexible polymer networks at short timescales have been studied in depth in a multitude of *in vitro* studies[10, 13, 26]. And many studies using more compliant cross-linkers showed that cross-links mechanics governed many short timescale rheological properties[8, 9, 14, 18, 19, 30]. More recent work has begun to highlight the long-timescale importance of transient cross-linking dynamics.[16, 17, 20, 33].

In these studies, long timescale creep behaviors are thought to arise predominantly from the transient nature of binding in most biologically relevant cross-linkers[17]. The importance of cross-link dynamics in determining the mechanical response of semi-flexible polymer networks has been known for at least 20 years[28]. Nevertheless, the dependence of network rheology on cross-link compliance and binding rates is still a subject of much research[21].

B. Overview of Theoretical Descriptions of Cross-linked Networks

A number of successful theoretical descriptions of cross-linked networks have been introduced into the literature[2, 11, 12, 25, 32]. For a comprehensive but straightforward introduction to this field we recommend [4]. We wish primarily to expand upon current theories of composite semi-flexible polymer and cross-link networks to incorporate both nonlinear extension and transient binding of cross-links.

Many theoretical methods have sought to model cross-link binding and unbinding directly[3, 21], and previous modeling work often take cross-links as extended springlike structures [15] separate from the main semi-flexible filament constituents. We simplify our approach to coarse-grained filaments which are able to slide past each other as molecular bonds form and rupture, akin to coarse-grained models of molecular friction[6, 23, 27]. This drag-like coupling has been shown to be an adequate approximation in the case of ionic cross-linking of actin[5, 29], and can be found in the theoretical basis of force-velocity curves for myosin bound filaments[1]. We propose that it will form a suitable bulk approximation in the presence of super molecular cross-links as well.

Importantly, this simplification allows us to extend our single polymer models to dynamical systems of larger network models for direct comparison between theory and modeling results. This level of coarse graining will therefore make it easier to understand classes of behavior for varying compositions of cross-linked filament networks. In addition, it gives concrete predictions for behaviors in widely different networks with measurable dependencies on molecular details.

II. EXPLANATION OF MODEL

A. Composite Cross-link & Filament Representation

We consider individual semi-flexible polymers as chains of springs of relaxed length l_s, whose orientations are linearly coupled to their neighbors. Filaments can be represented as a sequence of nodes with nearest neighbor interactions of the form

$$|F_{i,i+1}| = \mu \frac{|\mathbf{x_{i+1}} - \mathbf{x_i}| - l_s}{l_s}$$

$$a = b \quad (1)$$

This is essentially a discretized equivalent to a model of filaments with separable extensional and bending moduli like the type in [11] with a potential defined by

$$\mathcal{H} = \frac{1}{2}\kappa \int ds (\nabla^2 \mathbf{u})^2 + \frac{1}{2}\mu \int ds \left(\frac{dl(s)}{ds}\right)^2 \quad (2)$$

where, μ represents an extensional modulus of a filament, and κ represents a bending modulus.

Here, the extensional and bending moduli are taken as composite quantities related to both filament and cross-linker compliance in a manner similar to a recently proposed effective medium theory[2]. We provide a molecular level derivation of this composite compliance in Appendix B, but for now we wish to highlight the main features.

In the limit of highly rigid cross-links and flexible filaments, our model clearly reduces to the pure semi-flexible filament models of [11, 31]. In the opposite regime of nearly rigid filaments and highly flexible cross links, our method is still largely similar to the model of [2] in small strain regimes before any nonlinear cross link stiffening. However, in departure from those models, the magnitude of the force on interior cross-links in our model is still the same as those on the exterior. This is a simplification of the varying levels of strain that would actually be present in these cross-linkers, but we choose to ignore the slight variation in favor of an approximate, universal approach. Finally, in the event that the induced strain of the filament and the cross-linker are of comparable scales, our composite stiffness can be expressed by the approximation *huh* as we shown in Appendix B.

In our simulations we explore the role that nonlinear stiffening of filaments or cross linkers would play, and what complications arise.

B. 2D Network Formation

We are using a minimal network (Mikado model) of connected unstressed linear filaments in a rectangular 2D domain. We generate 2D networks of these semi-flexible filaments by laying down straight lines of length, L, with random position and orientation. We then assume that some fixed fraction of overlapping filaments become cross-linked (defined in II C) at their point of overlap.

Although real cytoskeletal networks may form with non-negligible anisotropy, we choose to focus our attention on isotropically initialized networks for simplicity. We define the density using the average distance between cross-links along a filament, l_c. A simple geometrical argument can be used to derive the number of filaments filling a domain as a function of L and l_c[11]. However, for our purposes we take the approximation that the number of filaments needed to tile a rectangular domain of size $W \times H$ is $2WH/Ll_c$, and that the length density is therefore $1/l_c$.

In the absence of cross-link slip, we expect the network to comprise a connected solid with a well defined elastic modulus[11, 31]. These networks are only well-connected when the ratio of filament length to intercrosslink spacing, L/l_c is greater than ~ 6. Near this percolation threshold, there are only locally connected domains, and discussions of global network properties becomes less reasonable. Additionally, as the filament density is increased beyond this point, there is another transition between non-affine bending and affine stretching of filaments, which changes the dominating term of the elastic modulus.

C. Drag-like Coupling Between Overlapping Filaments

In departure from the previous models, we wish to incorporate relaxation of the networks stored stress by letting the attachment points slip. We do this by introducing a drag-like coupling between filaments.

$$\mathbf{F_{drag}} = \xi \cdot \int ds\, (\mathbf{v(s)} - \mathbf{v_0(s)})\, f(s) \tag{3}$$

Where $f(s)$ represents the locational distribution of cross-link points (equal to 1 at locations of cross-links and 0 elsewhere). This model assumes a linear relation between applied force and the velocity difference between attached filaments. Obviously, non-linearities can arise in the presence of stretch dependent attachment kinetics as well as non-linear force extension of cross-links. In particular, we address non-linear effects of stress induced unbinding in Appendix A. Assuming inhomogeneities from non-linear effects are of second order, the motion for the entire network is governed by a dynamical equation of the form

$$\int ds\, (\zeta \mathbf{v_i(s)} + \xi \sum_j (\mathbf{v_i(s)} - \mathbf{v_j(s)})\, p_{ij}(s)) = \nabla \mathcal{H}_i \tag{4}$$

Here, the first term in the integral is the filament's intrinsic drag through its embedding fluid, ζ, while the second comes from the drag-like coupling between filaments, ξ.

III. ANALYTICAL DERIVATIONS

A. Low Strain Approximation of Effective Viscosity

We would like to begin with a calculation of a low-strain estimate of the effective viscosity for a network described by our model. We carry this out by assuming we can apply a constant stress along a transect of the network. With moderate stresses, we assume the network reaches a steady state affine creep. In this situation, we would find that the stress in the network exactly balances the sum of the drag-like forces from cross-link slip. So for any transect of length D, we have a force balance equation.

$$\sigma = \frac{1}{D} \sum_{filaments} \sum_{crosslinks} \xi \cdot (\mathbf{v_i} - \mathbf{v_0}) \tag{5}$$

where $\mathbf{v_i}(\mathbf{s}) - \mathbf{v_j}(\mathbf{s})$ is the difference between the velocity of a filament at it's cross-link point and the velocity of the filament to which it is a attached. We can convert the sum over cross-links to an integral over the length using the average density of cross-links, $1/l_c$ and invoking the assumption of (linear order) affine strain rate, $\mathbf{v_i} - \mathbf{v_0} = \dot{\gamma} x$. This results in

$$\begin{aligned}\sigma &= \frac{1}{D} \sum_{filaments} \xi \cdot \int_0^L ds\, (\mathbf{v}(\mathbf{s}) - \mathbf{v_0}(\mathbf{s}))\, \frac{1}{l_c} \\ &= \sum_{filaments} \frac{\xi \dot{\gamma} L}{l_c} \cos\theta \cdot (x_l + \frac{L}{2}\cos\theta)\end{aligned} \tag{6}$$

Here we have introduced the variables x_l, and θ to describe the leftmost endpoint and the angular orientation of a given filament respectively. Next, to perform the sum over all filaments we wish to convert this to an integral over all orientations and endpoints that intersect our line of stress. The max distance for the leftmost endpoint is the length of a filament, L, and the maximum angle as a function of endpoint is $\arccos(x_l/L)$. The linear density of endpoints is the constant $D/l_c L$ so our integrals can be rewritten as this density over x_l and θ between our maximum and minimum allowed bounds.

$$\sigma = \frac{1}{D} \int_0^L dx_l \int_{-\arccos(\frac{x_l}{L})}^{\arccos(\frac{x_l}{L})} \frac{d\theta}{\pi} \frac{\xi \dot{\gamma} L}{l_c} \cdot \frac{D}{L l_c} \cdot (x_l \cos\theta + \frac{L}{2} cos^2\theta) \tag{7}$$

Carrying out the integrals and correcting for dangling filament ends leaves us with a relation between stress and strain rate.

$$\sigma = \frac{(L - 2l_c)^2 \xi}{4\pi l_c^2} \dot{\gamma} \tag{8}$$

We recognize that the term next to the strain rate is the effective viscosity η_{eff} at steady state creep. (Result1, Say something about this)

B. Transient Softening from Filament Alignment

This will remain valid as long as any ordering by the induced strain is small relative to randomization by thermal motion. However, if the network reorganization is relatively fast, we find that our approximation no longer holds. Under shear there is a non-linear softening of the material due to a combination of reorientation and filament stretching. This non-linear softening actually decays away as network strain relaxes leading to a less than linear time dependence in the creep response curves. AND NEXT I FILL IN THE GAP FOR THE REORDERING PART

C. Longterm Network Tearing

For extensional stresses, the simple form of the effective viscosity simply picks up a different geometrical factor out front. In addition, extension stress induces a network thinning that takes place at a rate

$$\frac{\partial l_c}{dt} = l_c \dot{\gamma} = \frac{l_c \sigma}{\eta} \sim l_c^3 \frac{\sigma}{L^2 \xi} \tag{9}$$

We can see that the rate of network thinning accelerates as we would expect. When the network reaches some minimum connectivity we assume that it stops behaving as a continuum material and the network tears irreversibly.

$$\tau_{break} = \frac{\eta_{eff}}{2\sigma} \cdot \left(1 - \frac{l_c^2}{l_{break}^2}\right) \tag{10}$$

This provides us with an estimate of the timescale of catastrophic breakdown for a network with a given initial architecture and molecular drag.

D. Frequency Dependence of Elastic Modulus

Finally, we wish to extend this analysis to have some idea of the frequency dependence of the complex elastic modulus. I sure hope there is some way to do this.

IV. ANALYSIS OF SIMULATION RESULTS

Next, we wanted to test our analytical conclusions on a computational model. The technical details of the model can be found in the Appendix, but we summarize the main modeling points here.

A. Computational Simulation Method

For computational simplicity in these models, we assume that the bending rigidity, κ, is infinite, allowing us to model filaments as non-bending springs of rest length, L, and spring modulus μ. In the appendix, we show that our result is not significantly different from the result for semi-flexible polymers.

We discretize the filaments such that the equations of motion becomes a coupled system of equations for the velocities of filament endpoints, $\mathbf{x}$. The drag-like force between overlapping filaments results in a coupling of the velocities of endpoints.

$$\mathbf{A} \cdot \dot{\mathbf{x}} = \mathbf{f}(\mathbf{x}) \tag{11}$$

where $\mathbf{A}$ represents a coupling matrix between endpoints of filaments that overlap, and $\mathbf{f}(\mathbf{x})$ is the spring force between two endpoints. We can then numerically integrate this system of equations to find the time evolution of the positions of all filament endpoints.

We generate a network by laying down filaments with random position and orientation within a domain of size $2D$ by D with periodic boundaries. The external stress (shear or extensional/compressional) is applied to all filament endpoints falling within a fixed x-distance from the center of the domain. Finally, filament endpoints falling within a fixed x-distance from the edges of the domain are constrained to be nonmoving.

The nominal units for length, force, and time are μm, nN, and s, respectively. We explored parameters space around an estimate of biologically relevant parameter values,

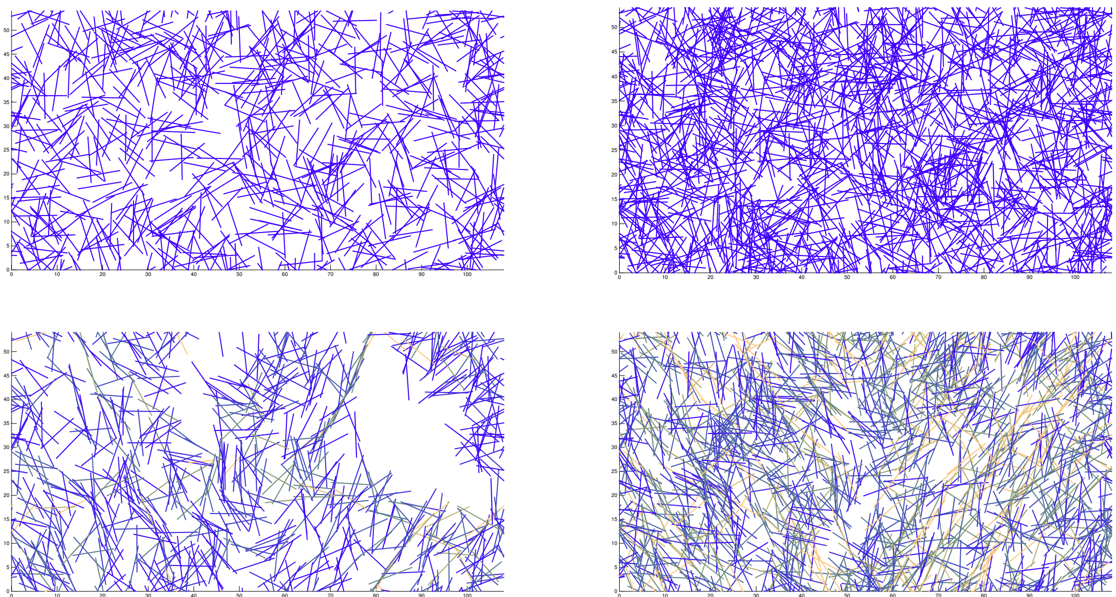

FIG. 1. Two Simulation setups with $L = 9\mu m, D = 54\mu m$ before and after 1000s of applied stress. a) low density $l_c = 2\mu m$, b) moderate density $l_c = 1\mu m$

given in Table X.

All changes in the force felt by an endpoint are made smooth to allow integration of the differential equation (i.e. moving between stress domains, constraint domains, and overlap coupling occurs smoothly to prevent discontinuities). Parameter conditions that cause instabilities are excluded, and the endpoint trajectories are integrated out to at least 1000 seconds. In addition, because we wish to probe the behavior of large scale network deformations, we are neglecting the sub-dominant effects from small thermal fluctuations.

B. Behavior at Moderate Strains above Percolation Limit

Beginning with moderate strains, our computational simulations show that in the high density limit, our theoretical derivation is highly accurate at explaining the network behavior. As the density of the network approaches the breakdown limit, the effective viscosity diverges from our expected value. At the low connectivity limit, our expected viscosity goes to 0, but the medium viscosity begins to take over as we cross the percolation threshold.

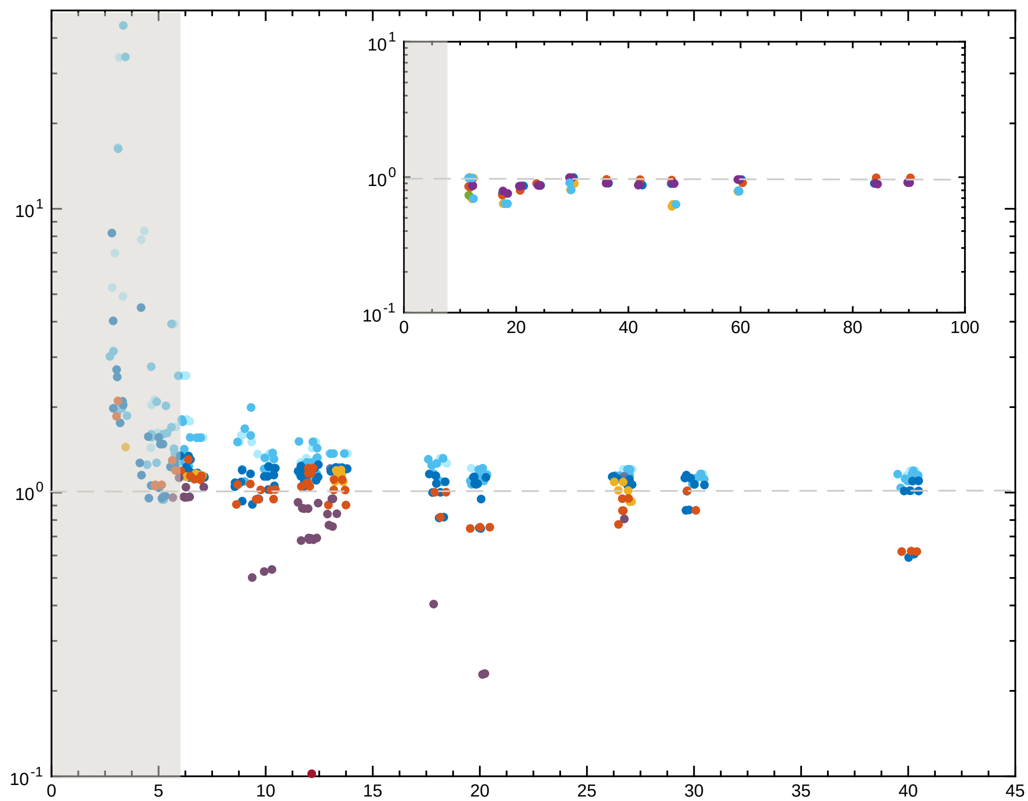

FIG. 2. Ratio of effective viscosity measured by shear simulation to predicted effective viscosity as a function of connectivity, L/l_c. Inset: Same measurement for extensional simulations

C. Behavior at High Shear Strain

up to moderate strains ($\gamma < 0.2$)

1. *Compliant Network, Low Cross-link Slip*

If the elastic deformation of the network is larger than the deformation from cross-link slip, the system enters a regime of transient network softening. Under these conditions, large scale reordering drives the network into a highly anisotropic distribution of filament orientations and lengths. As diagrammed in Figure, this reorientation causes there to be fewer bonds bridging the network perpendicular to the line of strain, which results in a lower connectivity as derived above.

The high levels of anisotropy are only transient, and cross-link slip relaxation actually brings the network back into a more uniform, unstrained steady-state. This causes the effective viscosity to decay back toward the isotropic limit over a time on the scale of ___. This gives rise to a less-than-linear creep response during times after pure elastic relaxation but before cross-link slip allows filament relaxation. In Figure , we show that the time dependent effective viscosity increases back toward the isotropic estimate as the slip-derived strain becomes of the same scale as that from pure mechanical stretching.

2. Rigid Network, High Cross-link Slip

However, if the deformation from cross-link slip begins to approach the order of the systems size

D. Tearing Events During Extensional Strain

This behavior is caused primarily by the low density network undergoing tearing events that interrupt global connectedness.

E. Subnetwork Formation from Nonlinear Filament Extension

F. Nonlinear Extension and Long-Lived Strain Memory

Finally, we found an interesting behavior when we introduced non-linear extensional stiffness into our filaments. This behavior mimics recent experiments in filamin cross-linked networks. Filamin provides a high level of compliance to a network ($\gamma_0 > 0.5$) without substantial cross-link unbinding. This allows large scale rearrangements to take place without driving very much cross-link slip similar to the conditions in section **??**. However, if we force individual filaments to undergo a strongly nonlinear stiffening at strains above 10%, we find an interesting long term "strain storage."

For moderate strains, this result is largely the same as the result for extensional stress. However, at larger deformations, extensional networks tear apart To further explore the occurrence of tearing events ...

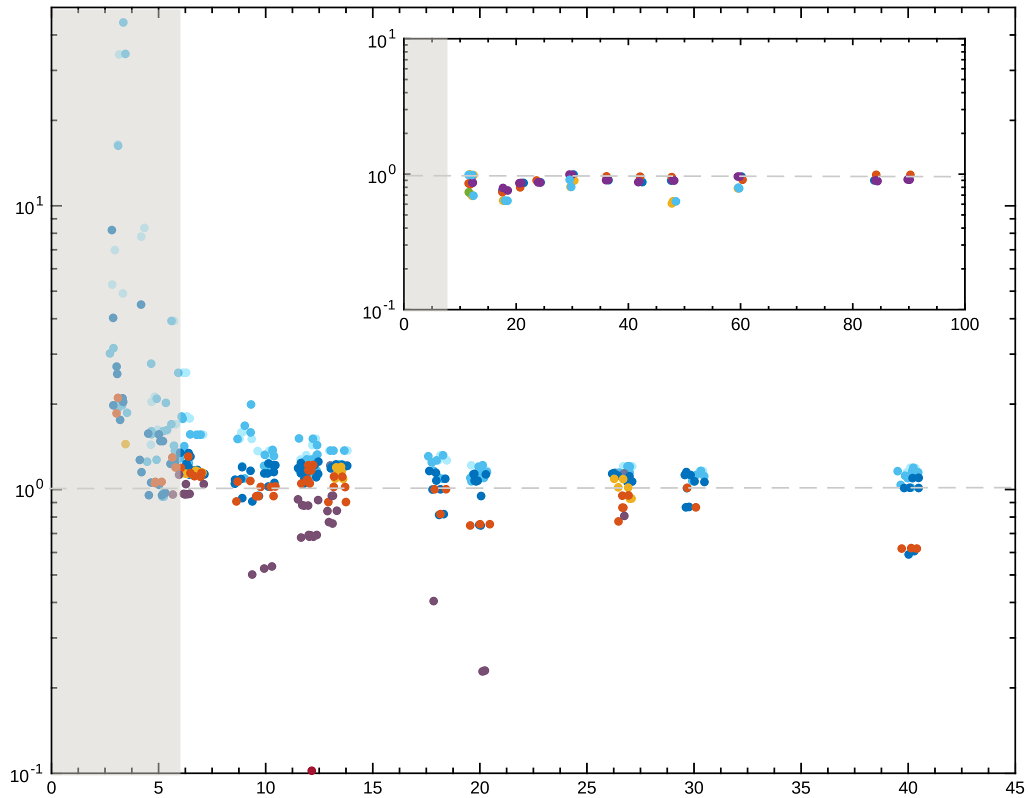

FIG. 3. Analysis of viscosity softening under large shear strain. Inset: time scaling of creep response vs relative filament compliance

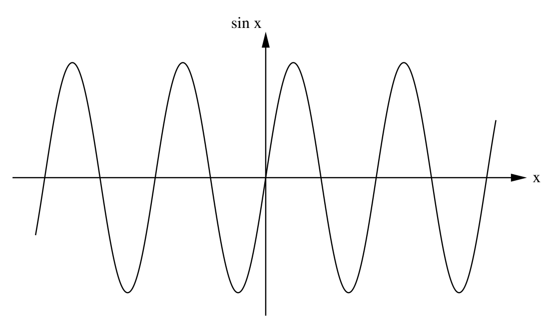

FIG. 4. Tearing rate as a function of L/l_c.

We explored a mode of deformation highly relevant to cortical mechanics in vivo. Under this deformation stress was applied between a region of extension and region of compression. Interestingly, until nearing the point of breakdown, the network did not experience a significant change in effective viscosity. This was due to the between the diminishing viscosity of the thinning domain and the increasing viscosity of the thickening domain.

Finally, we wished to explore the non-linear effects of reorientation of the filaments and non-linear network thinning/thickening. To do so, we applied oscillatory shear

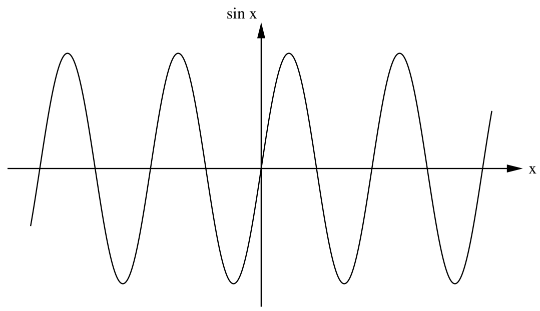

FIG. 5. Frequency dependence of elastic moduli.

V. DISCUSSION

Finally I wax philosophical, but who is going to pay for the ink?

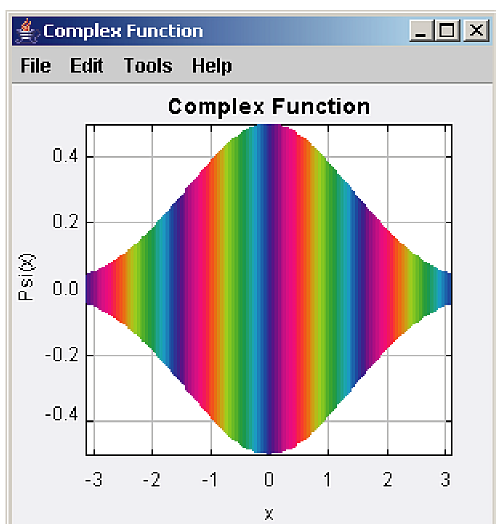

FIG. 6. Phase diagram of network connectivity.

Appendix A: Deriving Molecular Drag Coefficients

Thus far, the idea of a molecular drag coefficient was taken as a phenomenological, measured parameter for a given experimental setup. While this is a sufficient pragmatic justification, it's useful to try to motivate the quantitative value of this drag coefficient by connecting it to the underlying cross-link properties of binding affinity, concentration, and extensibility.

To do this we'll imagine the simplified case of two cross linkers sliding past each other in one dimension. In this case, imagine that we have an equilibrium number of bound cross-linkers, n_B, each of which can be displaced from its equilibrium length by some distance x. Each cross linker unbinds with rate k_{off} and rebinds at it's relaxed position ($x = 0$) with rate k_{on}. At the same time, all the cross linkers are being pulled from their relaxed position at a rate, v, which is simply the rate at which the filaments are sliding past each other.

We can right down an equation for the change in the density of cross-links as they are pulled upon, bind, and unbind.

$$\frac{\partial \rho}{\partial t} = -k_{off}\rho(x) - v\frac{\partial \rho}{\partial x} + k_{on}\delta(x) \tag{A1}$$

Recognizing that $\int \rho(x) = n_B$ implies $k_{on} = k_{off}n_B$, we can find the steady state solution

$$\rho(x) = \frac{n_b k_{off}}{v} \cdot exp\left(-\frac{k_{off}}{v}x\right) \tag{A2}$$

If each cross-link has a spring constant μ_c, then we can equate the force on all cross-links to the applied force that is sliding the filaments past each other. Realistically, the spring constant and binding affinity would be functions of the cross-link stretch, but here we are taking them as approximately constant.

$$\int_0^\infty \rho(x)\mu_c x dx = v\frac{\mu_c n_B}{k_{off}} = F_{app} \tag{A3}$$

Therefore, the term next to v, (i.e. $\frac{\mu_c n_B}{k_{off}}$) would be equal to our molecular drag coefficient, ξ. assuming, approximately 1-5 cross links per filament overlap, and using the following table of estimates pulled from Ferrer et al., we can chart the accuracy of this simple predictive model.

This molecular description assumed both a constant off-rate and linear force extension of cross-links. In the event that binding kinetics are regulated by the state of extension, we

cross-linker type	α-actinin	filamin-A
dissociation constant (s^{-1})	0.4	0.6
spring constant ($nN/\mu m$)	455	820
drag coefficient ($\frac{nN \cdot s}{\mu m}$)	200-1000	500-2500

would expect (based on Rf) to find a region that exhibits a stick-slip behavior instead of the smooth. Based on the coupling between cross-links this could either manifest itself as a global stick-slip behavior or as a heterogenous mixture of jammed and sliding cross-links. It would be interesting to explore this topic further in the future, but as neither phenomenon is observed experimentally, we choose to ignore these nonlinear effects for the time being.

Appendix B: Deriving Filament and Cross-Link Composite Extensional Modulus

Section describing how you derive the extensional modulus.

Appendix C: Semiflexibiliy

Brief section showing that the results are not thoroughly flummoxed by semi flexibility.

Appendix D: Simulation details

And I think I'll probably include all the gory details of how my simulations work since I'll be wanting to have direct references to the code.

```
double y0 = 10; // example of declaration and assignment statement
double v0 = 0;  // initial velocity
double t = 0;   // time
double dt = 0.01; // time step
double y = y0; // solved all problems
```

[1] Shiladitya Banerjee, M. Cristina Marchetti, and Kristian Müller-Nedebock. Motor-driven dynamics of cytoskeletal filaments in motility assays. *Phys. Rev. E*, 84:011914, Jul 2011.

[2] C. P. Broedersz, C. Storm, and F. C. MacKintosh. Effective-medium approach for stiff polymer networks with flexible cross-links. *Phys. Rev. E*, 79:061914, Jun 2009.

[3] Chase P. Broedersz, Martin Depken, Norman Y. Yao, Martin R. Pollak, David A. Weitz, and Frederick C. MacKintosh. Cross-link-governed dynamics of biopolymer networks. *Phys. Rev. Lett.*, 105:238101, Nov 2010.

[4] P. Broedersz, C. and C. MacKintosh, F.˙Modeling semiflexible polymer networks. *Rev. Mod. Phys.*, 86:995–1036, Jul 2014.

[5] Preethi L. Chandran and Mohammad R. K. Mofrad. Averaged implicit hydrodynamic model of semiflexible filaments. *Phys. Rev. E*, 81:031920, Mar 2010.

[6] A. E. Filippov, J. Klafter, and M. Urbakh. Friction through dynamical formation and rupture of molecular bonds. *Phys. Rev. Lett.*, 92:135503, Mar 2004.

[7] Daniel A. Fletcher and R. Dyche Mullins. Cell mechanics and the cytoskeleton. *Nature*, 463(7280):485–492, 01 2010.

[8] M. L. Gardel, F. Nakamura, J. Hartwig, J. C. Crocker, T. P. Stossel, and D. A. Weitz. Stress-dependent elasticity of composite actin networks as a model for cell behavior. *Phys. Rev. Lett.*, 96:088102, Mar 2006.

[9] M. L. Gardel, F. Nakamura, J. H. Hartwig, J. C. Crocker, T. P. Stossel, and D. A. Weitz. Prestressed f-actin networks cross-linked by hinged filamins replicate mechanical properties of cells. *Proceedings of the National Academy of Sciences of the United States of America*, 103(6):1762–1767, 2006.

[10] M. L. Gardel, J. H. Shin, F. C. MacKintosh, L. Mahadevan, P. Matsudaira, and D. A. Weitz. Elastic behavior of cross-linked and bundled actin networks. *Science*, 304(5675):1301–1305, 2004.

[11] David A. Head, Alex J. Levine, and F. C. MacKintosh. Deformation of cross-linked semiflexible polymer networks. *Phys. Rev. Lett.*, 91:108102, Sep 2003.

[12] Claus Heussinger, Boris Schaefer, and Erwin Frey. Nonaffine rubber elasticity for stiff polymer networks. *Phys. Rev. E*, 76:031906, Sep 2007.

[13] Paul A. Janmey, Soren Hvidt, Jennifer Lamb, and Thomas P. Stossel. Resemblance of actin-binding protein/actin gels to covalently crosslinked networks. *Nature*, 345(6270):89–92, 05 1990.

[14] K. E. Kasza, C. P. Broedersz, G. H. Koenderink, Y. C. Lin, W. Messner, E. A. Millman, F. Nakamura, T. P. Stossel, F. C. MacKintosh, and D. A. Weitz. Actin filament length tunes elasticity of flexibly cross-linked actin networks. *Biophysical Journal*, 99(4):1091–1100, 2015/03/12.

[15] Taeyoon Kim, Wonmuk Hwang, and Roger D Kamm. Dynamic role of cross-linking proteins in actin rheology. *Biophysical Journal*, 101(7):1597–1603, 10 2011.

[16] O. Lieleg, M. M. A. E. Claessens, Y. Luan, and A. R. Bausch. Transient binding and dissipation in cross-linked actin networks. *Phys. Rev. Lett.*, 101:108101, Sep 2008.

[17] O. Lieleg, K. M. Schmoller, M. M. A. E. Claessens, and A. R. Bausch. Cytoskeletal polymer networks: Viscoelastic properties are determined by the microscopic interaction potential of cross-links. *Biophysical Journal*, 96(11):4725–4732, 6 2009.

[18] Oliver Lieleg, Mireille M. A. E. Claessens, and Andreas R. Bausch. Structure and dynamics of cross-linked actin networks. *Soft Matter*, 6:218–225, 2010.

[19] Yi-Chia Lin, Chase P. Broedersz, Amy C. Rowat, Tatjana Wedig, Harald Herrmann, Frederick C. MacKintosh, and David A. Weitz. Divalent cations crosslink vimentin intermediate filament tail domains to regulate network mechanics. *Journal of Molecular Biology*, 399(4):637 – 644, 2010.

[20] J. Liu, G. H. Koenderink, K. E. Kasza, F. C. MacKintosh, and D. A. Weitz. Visualizing the strain field in semiflexible polymer networks: Strain fluctuations and nonlinear rheology of f-actin gels. *Phys. Rev. Lett.*, 98:198304, May 2007.

[21] Kei W. Müller, Robijn F. Bruinsma, Oliver Lieleg, Andreas R. Bausch, Wolfgang A. Wall, and Alex J. Levine. Rheology of semiflexible bundle networks with transient linkers. *Phys. Rev. Lett.*, 112:238102, Jun 2014.

[22] Guillaume Salbreux, Guillaume Charras, and Ewa Paluch. Actin cortex mechanics and cellular morphogenesis. *Trends in Cell Biology*, 22(10):536 – 545, 2012.

[23] Evan Spruijt, Joris Sprakel, Marc Lemmers, Martien A. Cohen Stuart, and Jasper van der Gucht. Relaxation dynamics at different time scales in electrostatic complexes: Time-salt superposition. *Phys. Rev. Lett.*, 105:208301, Nov 2010.

[24] Dimitrije Stamenovic. Cell mechanics: Two regimes, maybe three? *Nat Mater*, 5(8):597–598, 08 2006.

[25] Cornelis Storm, Jennifer J. Pastore, F. C. MacKintosh, T. C. Lubensky, and Paul A. Janmey. Nonlinear elasticity in biological gels. *Nature*, 435(7039):191–194, 05 2005.

[26] R. Tharmann, M. M. A. E. Claessens, and A. R. Bausch. Viscoelasticity of isotropically cross-linked actin networks. *Phys. Rev. Lett.*, 98:088103, Feb 2007.

[27] Andrea Vanossi, Nicola Manini, Michael Urbakh, Stefano Zapperi, and Erio Tosatti. *Colloquium* : Modeling friction: From nanoscale to mesoscale. *Rev. Mod. Phys.*, 85:529–552, Apr 2013.

[28] D.H. Wachsstock, W.H. Schwarz, and T.D. Pollard. Cross-linker dynamics determine the mechanical properties of actin gels. *Biophysical Journal*, 66(3, Part 1):801 – 809, 1994.

[29] Andrew Ward, Feodor Hilitski, Walter Schwenger, David Welch, A. W. C. Lau, Vincenzo Vitelli, L. Mahadevan, and Zvonimir Dogic. Solid friction between soft filaments. *Nat Mater*, advance online publication:–, 03 2015.

[30] Sabine M. Volkmer Ward, Astrid Weins, Martin R. Pollak, and David A. Weitz. Dynamic viscoelasticity of actin cross-linked with wild-type and disease-causing mutant -actinin-4. *Biophysical Journal*, 95(10):4915 – 4923, 2008.

[31] Jan Wilhelm and Erwin Frey. Elasticity of stiff polymer networks. *Phys. Rev. Lett.*, 91:108103, Sep 2003.

[32] M. Wyart, H. Liang, A. Kabla, and L. Mahadevan. Elasticity of floppy and stiff random networks. *Phys. Rev. Lett.*, 101:215501, Nov 2008.

[33] Norman Y. Yao, Daniel J. Becker, Chase P. Broedersz, Martin Depken, Frederick C. MacKintosh, Martin R. Pollak, and David A. Weitz. Nonlinear viscoelasticity of actin transiently cross-linked with mutant -actinin-4. *Journal of Molecular Biology*, 411(5):1062 – 1071, 2011.